Runx2 and Runx3 are essential for chondrocyte maturation, and Runx2 regulates limb growth through induction of *Indian hedgehog*

Carolina A. Yoshida,[1,2,7] Hiromitsu Yamamoto,[3,7] Takashi Fujita,[4] Tatsuya Furuichi,[1] Kosei Ito,[5] Ken-ichi Inoue,[5] Kei Yamana,[6] Akira Zanma,[1,6] Kenji Takada,[2] Yoshiaki Ito,[5] and Toshihisa Komori[1,8]

[1]Department of Molecular Medicine, Osaka University Graduate School of Medicine, Suita, Osaka 565-0871, Japan; [2]Department of Orthodontics and Dentofacial Orthopedics, Osaka University Faculty of Dentistry, Suita, Osaka 565-0871, Japan; [3]Department of Oral and Maxillofacial Surgery, Graduate School of Medicine, Kyoto University, Sakyo, Kyoto 606-8507, Japan; [4]Department of Pharmacology, Faculty of Pharmaceutical Science, Setsunan University, Hirakata, Osaka, Japan; [5]Insitute of Molecular and Cell Biology, Singapore 117609, Singapore; [6]Teijin Institute for Biomedical Research, Teijin Ltd., Hino, Tokyo 191-8512, Japan

The differentiation of mesenchymal cells into chondrocytes and chondrocyte proliferation and maturation are fundamental steps in skeletal development. Runx2 is essential for osteoblast differentiation and is involved in chondrocyte maturation. Although chondrocyte maturation is delayed in *Runx2*-deficient (*Runx2*$^{-/-}$) mice, terminal differentiation of chondrocytes does occur, indicating that additional factors are involved in chondrocyte maturation. We investigated the involvement of Runx3 in chondrocyte differentiation by generating *Runx2*-and-*Runx3*-deficient (*Runx2*$^{-/-}$*3*$^{-/-}$) mice. We found that chondrocyte differentiation was inhibited depending on the dosages of *Runx2* and *Runx3*, and *Runx2*$^{-/-}$*3*$^{-/-}$ mice showed a complete absence of chondrocyte maturation. Further, the length of the limbs was reduced depending on the dosages of *Runx2* and *Runx3*, due to reduced and disorganized chondrocyte proliferation and reduced cell size in the diaphyses. *Runx2*$^{-/-}$*3*$^{-/-}$ mice did not express Ihh, which regulates chondrocyte proliferation and maturation. Adenoviral introduction of *Runx2* in *Runx2*$^{-/-}$ chondrocyte cultures strongly induced *Ihh* expression. Moreover, Runx2 directly bound to the promoter region of the *Ihh* gene and strongly induced expression of the reporter gene driven by the *Ihh* promoter. These findings demonstrate that Runx2 and Runx3 are essential for chondrocyte maturation and that Runx2 regulates limb growth by organizing chondrocyte maturation and proliferation through the induction of *Ihh* expression.

[*Keywords*: Runx2; Runx3; chondrocyte proliferation; chondrocyte maturation; Ihh]

Received December 2, 2003; revised version accepted March 11, 2004.

Vertebrate skeletons are constructed through the formation of bone structures, a process that is achieved by intramembranous or endochondral ossification. Intramembranous bones, which are directly formed by osteoblasts, are restricted to the cranial vault, some facial bones, and parts of the mandible and clavicle, whereas the rest of the skeleton is composed of endochondral bones that are formed as a cartilaginous template which is then replaced by bone. In early skeletal development, mesenchymal cells condense and acquire the phenotypes of chondrocytes including the ability to produce Col2a1 and proteoglycan. In the process of endochondral ossification, immature chondrocytes proliferate, and chondrocytes at the center of the cartilaginous skeleton begin to mature to become prehypertrophic chondrocytes, which express parathyroid hormone/parathyroid hormone-related peptide (*Pthlh*) receptor (*Pthr1*) and Indian hedgehog (*Ihh*). The prehypertrophic chondrocytes further mature to hypertrophic chondrocytes, which express *Col10a1*. Upon the terminal differentiation of chondrocytes, the terminal hypertrophic chondrocytes express *osteopontin*, the matrix is mineralized, vascular vessels invade the calcified cartilage, and finally the cartilage is replaced by bone. Chondrocyte proliferation and differentiation occur in an organized manner and result in the formation of a growth plate that is composed of layers of chondrocytes at different stages of differentiation, in-

[7]These authors contributed equally to this work.
[8]Corresponding author.
E-MAIL komorit@imed3.med.osaka-u.ac.jp; FAX 81-6-6879-7796.
Article and publication are at http://www.genesdev.org/cgi/doi/10.1101/gad.1174704.

cluding resting, proliferating, prehypertrophic, hypertrophic, and terminal hypertrophic chondrocytes (Gilbert 1997; Inada et al. 1999).

Ihh plays important roles in the formation of the growth plate. Ihh induces *Pthlh* expression at the epiphysial surface, probably through indirect pathways. The expression of *Pthlh* at the epiphysial surface results in a gradient of Pthlh with decreasing levels towards the diaphysis, and inhibits chondrocyte maturation through Pthr1 (Vortkamp et al. 1996). The limbs of $Ihh^{-/-}$ mice are severely diminished due to reduced chondrocyte proliferation, indicating that Ihh promotes chondrocyte proliferation (St-Jacques et al. 1999). Therefore, Ihh regulates both the maturation and proliferation of chondrocytes.

Runx2 (runt-related transcription factor 2) is a transcription factor that belongs to the Runx family (Komori 2002) and acquires DNA binding activity by heterodimerizing with Cbfβ (Kundu et al. 2002; Miller et al. 2002; Yoshida et al. 2002). $Runx2^{-/-}$ mice die just after birth and completely lack bone formation due to the absence of osteoblast differentiation, demonstrating that Runx2 is essential for osteoblast differentiation (Komori et al. 1997; Otto et al. 1997). Further, chondrocyte maturation is delayed in $Runx2^{-/-}$ mice (Inada et al. 1999; Kim et al. 1999), Runx2 promotes chondrocyte maturation (Enomoto et al. 2000; Takeda et al. 2001; Ueta et al. 2001; Stricker et al. 2002), dominant-negative Runx2 inhibits chondrocyte maturation (Ueta et al. 2001; Stricker et al. 2002), and the overexpression of *Runx2* in chondrocytes restores the chondrocyte maturation in $Runx2^{-/-}$ mice (Takeda et al. 2001). However, chondrocyte maturation to the terminal stage does eventually occur in $Runx2^{-/-}$ mice (Komori et al. 1997; Otto et al. 1997; Inada et al. 1999; Kim et al. 1999), indicating that Runx2 is not essential for chondrocyte maturation and that other factors are involved in chondrocyte maturation.

Runx3, which also belongs to the Runx family, plays important roles in the growth regulation of gastric epithelial cells and the development of dorsal root ganglion neurons (Inoue et al. 2002; Levanon et al. 2002; Li et al. 2002). As *Runx3* is expressed in the cartilage (Levanon et al. 2001; Stricker et al. 2002), we investigated the involvement of Runx3 in chondrocyte differentiation by generating $Runx2^{-/-}3^{-/-}$ mice. Chondrocyte maturation was mildly delayed in $Runx3^{-/-}$ mice during embryogenesis, but it was completely absent in $Runx2^{-/-}3^{-/-}$ mice, demonstrating that Runx2 and Runx3 are functionally redundant in chondrocytes and play an essential role in chondrocyte maturation. $Runx2^{-/-}3^{-/-}$ mice, which completely lacked *Ihh* expression, had severely shortened limbs due to reduced and disorganized chondrocyte proliferation and reduced cell size in the diaphyses. Further, the introduction of *Runx2* to $Runx2^{-/-}$ chondrocytes induced *Ihh* expression, and Runx2 directly regulated the *Ihh* promoter. These findings indicate that Runx2 is also involved in chondrocyte proliferation, and that Runx2 coordinates chondrocyte maturation and proliferation by regulating *Ihh* expression.

Results

Runx3 *expression in the skeleton*

We examined *Runx3* expression in the skeleton of $Runx3^{+/-}$ mice during embryogenesis using the β-galactosidase gene, which was integrated in exon 3 of *Runx3* in $Runx3^{+/-}$ mice (Li et al. 2002), followed by detection of β-galactosidase activity (Fig. 1). *Runx3* expression was first detected in the skeleton at embryonic day E12.5 (E12.5) in the scapulae, ribs, and skeletal parts of the limbs (Fig. 1A,D). *Runx3* expression extended to the pelvic bones and vertebrae at E13.5 (Fig. 1B,E), and to most of the cartilaginous skeletons at E15.5 (Fig. 1C,F). The level of *Runx3* expression increased at the stage of prehypertrophic chondrocytes and was maintained in hypertrophic chondrocytes, but it decreased in terminal hypertrophic chondrocytes (Fig. 1G,H). The expression patterns were compatible with the previous findings, which were obtained by in situ hybridization (Stricker et al. 2002).

Delayed endochondral ossification in $Runx3^{-/-}$ *and* $Runx2^{+/-}3^{-/-}$ *mice*

Although $Runx3^{+/-}$ mice develop normally, $Runx3^{-/-}$ mice of the C57BL/6 background die shortly after birth (Li et al. 2002). In $Runx3^{-/-}$ embryos, chondrocyte maturation and vascular invasion into the cartilage were slightly delayed at E15.5 (Fig. 1I–L), although the mice showed grossly normal skeletal development at the neonatal stage (Fig. 2B; data not shown). To further investigate the involvement of Runx3 in skeletal development, we mated $Runx3^{+/-}$ mice with $Runx2^{+/-}$ mice, and finally we generated $Runx2^{-/-}3^{-/-}$ mice. Although $Runx2^{+/-}$ mice achieved grossly normal endochondral ossification at the newborn stage (Komori et al. 1997; Otto et al. 1997; data not shown), endochondral ossification was clearly delayed in the $Runx2^{+/-}3^{-/-}$ mice, as shown by the smaller mineralized regions in the chondrocranium, vertebrae, ribs, and limbs at the newborn stage (Fig. 2C; data not shown). In the tibiae of wild-type and $Runx3^{-/-}$ mice at E18.5, the cartilage was largely replaced by bone (Fig. 2D,E). However, in the $Runx2^{+/-}3^{-/-}$ tibiae, the diaphyses were composed of calcified cartilage that was covered with the bone collar, blood vessels had just started to invade the calcified cartilage, and no trabecular bone was observed (Fig. 2F). These features of the $Runx2^{+/-}3^{-/-}$ tibiae were apparently caused by delayed chondrocyte maturation because the expression of *Pthr1*, *Ihh*, *Col10a1*, and *osteopontin* were restricted to the diaphyses (Fig. 2L,O; data not shown). These findings indicate that Runx3 is required for endochondral ossification if the *Runx2* gene dosage is halved.

Mildly delayed early skeletal development in $Runx2^{-/-}3^{-/-}$ *embryos*

In the early skeletal development in $Runx2^{-/-}3^{-/-}$ embryos, chondrocyte differentiation and proteoglycan pro-

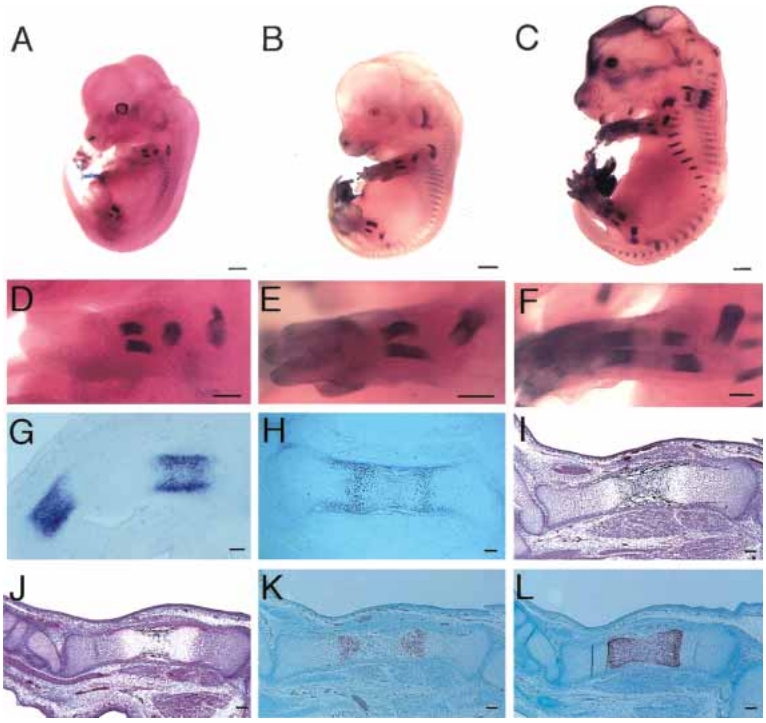

Figure 1. *Runx3* expression in *Runx3*$^{+/-}$ mice and skeletal development in *Runx3*$^{-/-}$ mice during embryogenesis. (*A–H*), *Runx3* expression in *Runx3*$^{+/-}$ mice at E12.5 (*A,D,G*), E13.5 (*B,E*), E15.5 (*C,F*) and E16.5 (*H*). We examined *Runx3* expression by the activity of β-galactosidase, whose gene had been integrated in exon 3 of *Runx3*, in *Runx3*$^{+/-}$ mice. (*A–F*) *Runx3* was expressed in cartilaginous skeletons. (*G,H*) *Runx3* was specifically expressed in chondrocytes but not in osteoblasts in the skeleton, and its expression was up-regulated in prehypertrophic chondrocytes and down-regulated in terminal hypertrophic chondrocytes. (*I–L*) Skeletal development in *Runx3*$^{-/-}$ mice at E15.5. H&E and Kossa staining (*I,J*) and in situ hybridization using *Col10a1* antisense probe (*K,L*) of wild-type (*I,K*) and *Runx3*$^{-/-}$ (*J,L*) tibiae. Calcification was stained black in *I* and *J*. We detected no signal using a sense probe of *Col10a1* (data not shown). The diaphyses of wild-type tibiae were composed of calcified cartilage that was negative for *Col10a1* expression (*K*), and blood vessels had invaded the diaphyses (*I*). (*J,L*) The diaphyses of *Runx3*$^{-/-}$ tibiae were composed of *Col10a1*-positive hypertrophic chondrocytes without vascular invasion. Bars: *A–C*, 1 mm; *D–F*, 500 μm; *G–L*, 100 μm.

duction seemed to be mildly delayed (Fig. 3A–F). Cartilaginous anlagen was clearly seen in the wild-type and *Runx2*$^{-/-}$ embryos but not in the *Runx2*$^{-/-}$*3*$^{-/-}$ embryos at E12.5, indicating that chondrocyte differentiation was mildly delayed in *Runx2*$^{-/-}$*3*$^{-/-}$ embryos (Fig. 3A–C). Alcian blue staining of E13.5 *Runx2*$^{-/-}$*3*$^{-/-}$ embryos was weaker than that of the wild-type and *Runx2*$^{-/-}$ embryos, indicating less proteoglycan production in *Runx2*$^{-/-}$*3*$^{-/-}$ cartilage, which was probably due to delayed chondrocyte differentiation (Fig. 3D–F). As to *Sox9* expression, which is essential for mesenchymal condensation (Bi et al. 1999), within the limb skeletons of E13.5 wild-type and *Runx2*$^{-/-}$ embryos, there was strong expression in the skeletal parts with immature chondrocytes, but weak expression in the skeletal parts with differentiating chondrocytes (Fig. 3G,H,J,K). In the limb skeletons of *Runx2*$^{-/-}$*3*$^{-/-}$ embryos at E13.5, however, all chondrocytes strongly expressed *Sox9* (Fig. 3I,L), indicating that all of the chondrocytes were immature. As *Ihh* is expressed in chondrocytes at an early stage of skeletal development (Bitgood and McMahon 1995), we examined *Ihh* expression at E12.5 and E13.5. *Ihh* was expressed in immature chondrocytes in *Runx2*$^{-/-}$*3*$^{-/-}$ mice as well as in wild-type and *Runx2*$^{-/-}$ mice, although the appearance of *Ihh* expression was slightly delayed in *Runx2*$^{-/-}$*3*$^{-/-}$ mice (Fig. 3M–R). This indicates that neither Runx2 nor Runx3 is essential for the *Ihh* expression at the early stage of skeletal development. These findings indicate that Runx2 and Runx3 are not essential for, but are partly involved in early chondrocyte differentiation and that they begin to induce chondrocyte differentiation as soon as mesenchymal condensation is completed.

Complete absence of chondrocyte maturation in Runx2$^{-/-}$3$^{-/-}$ *mice*

Mineralization, which is observed in restricted regions of the limbs, vertebrae, and ribs of *Runx2*$^{-/-}$ newborns, was completely absent throughout the entire skeletons of both *Runx2*$^{-/-}$*3*$^{+/-}$ and *Runx2*$^{-/-}$*3*$^{-/-}$ newborns (Fig. 4). Histological analyses of *Runx2*$^{-/-}$ tibiae at E18.5 showed that the diaphyses were composed of calcified cartilage, and the chondrocytes in the metaphyses expressed *Pthr1*, *Ihh*, or *Col10a1* on in situ hybridization (Fig. 5). The level of *Ihh* expression in *Runx2*$^{-/-}$ limbs at E18.5 was less than one-third of that in wild-type limbs on real-time RT–PCR analysis (see Fig. 7A, below). In the tibiae of *Runx2*$^{-/-}$*3*$^{+/-}$ and *Runx2*$^{-/-}$*3*$^{-/-}$ embryos at E18.5, however, there was no mineralization, and all of the chondrocytes expressed *Col2a1* but not *Col10a1* (Fig. 5). *Pthr1* and *Ihh* expression were very weakly detected in the diaphyses of *Runx2*$^{-/-}$*3*$^{+/-}$ tibiae, but were not detected in *Runx2*$^{-/-}$*3*$^{-/-}$ tibiae (Fig. 5K,L,O,P). The absence of *Ihh* and *Col10a1* expression in *Runx2*$^{-/-}$*3*$^{-/-}$ limbs was confirmed by real-time RT–PCR (see Fig. 7A,B, below). The chondrocytes in the diaphyses of *Runx2*$^{-/-}$*3*$^{+/-}$ tibiae at E18.5 were slightly enlarged, whereas the chondrocytes throughout the *Runx2*$^{-/-}$*3*$^{-/-}$ tibiae were homogeneously small (Fig. 6C,D). We observed that there was complete maturational blockage of chondrocytes throughout the entire skeletons of *Runx2*$^{-/-}$*3*$^{-/-}$ embryos at E18.5 (data not shown). These findings indicate that the degree of maturational blockage of chondrocytes is dependent on the dosages of *Runx2* and *Runx3*, and demonstrate that Runx2 and/or Runx3 must be present for chondrocyte maturation to occur.

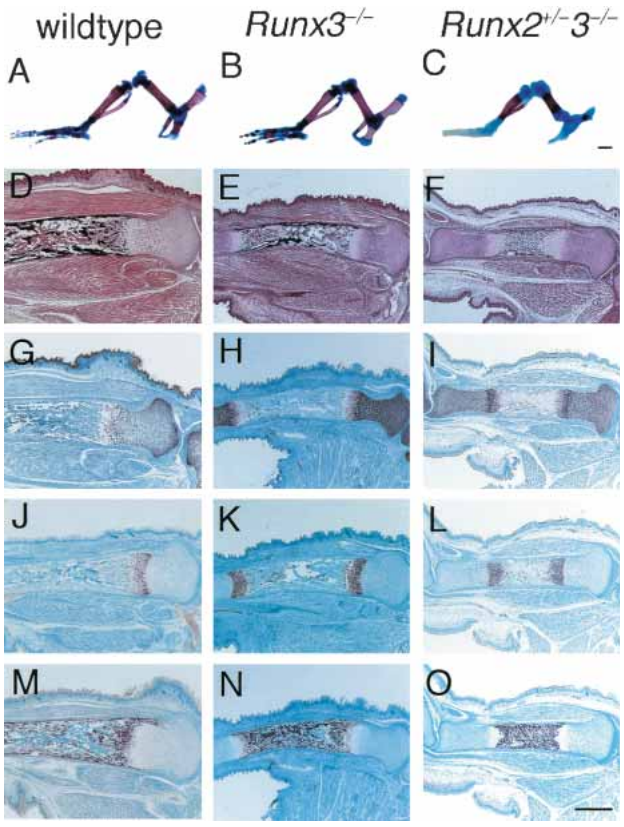

Figure 2. Skeletal development in *Runx3*$^{-/-}$ and *Runx2*$^{+/-}$*3*$^{-/-}$ mice. (*A–C*) Hind limb skeletons of wild-type (*A*), *Runx3*$^{-/-}$ (*B*), and *Runx2*$^{+/-}$*3*$^{-/-}$ (*C*) newborns. Calcified tissues were stained red with Alizarin red, and cartilage was stained blue with Alcian blue. Wild-type and *Runx3*$^{-/-}$ limb skeletons showed a similar pattern of mineralization (*A*,*B*), whereas the mineralized regions of *Runx2*$^{+/-}$*3*$^{-/-}$ limbs were much smaller (*C*). (*D–F*) Histological analysis of the tibiae of wild-type (*D*), *Runx3*$^{-/-}$ (*E*), and *Runx2*$^{+/-}$*3*$^{-/-}$ (*F*) embryos at E18.5. The sections were stained with H&E and Kossa. (*G–O*) In situ hybridization using the antisense probes of *Col2a1* (*G–I*), *Col10a1* (*J–L*), and *osteopontin* (*M–O*). We detected no signal using sense probes of *Col2a1*, *Col10a1*, or *osteopontin* (data not shown). In the tibiae of wild-type and *Runx3*$^{-/-}$ embryos, the cartilage was largely replaced by bone (*D*,*E*), *osteopontin*-positive osteoblasts occupied the bone marrow (*M*,*N*), and *Col2a1*-positive (*G*,*H*) or *Col10a1*-positive (*J*,*K*) chondrocytes were observed in the epiphyses. *Runx2*$^{+/-}$*3*$^{-/-}$ tibiae were still cartilaginous (*F*), and the chondrocytes expressed *Col2a1* (*I*) or *Col10a1* (*L*) except for those in the mineralized diaphyses, which were occupied by *osteopontin*-positive terminal hypertrophic chondrocytes (*O*). Bars: *A–C*, 1 mm; *D–O*, 500 μm.

Reduced and disorganized chondrocyte proliferation in Runx2$^{-/-}$3$^{-/-}$ *limb skeletons*

The limbs of *Runx2*$^{-/-}$*3*$^{-/-}$ embryos at E13.5 were slightly shorter than those of wild-type and *Runx2*$^{-/-}$ embryos (Fig. 3D–F), and the limb length was apparently reduced in the *Runx2*$^{-/-}$ and *Runx2*$^{-/-}$*3*$^{-/-}$ newborns according to the dosages of *Runx2* and *Runx3* (Fig. 4I–L). This suggested that the reduction in limb length was coupled with inhibition of chondrocyte maturation. We labeled proliferating chondrocytes with BrdU and examined the relationship between chondrocyte proliferation and maturation of limb skeletons (Fig. 6). The chondrocytes in *Runx2*$^{-/-}$ tibiae differentiated to the terminal stage, and all stages of chondrocyte maturation were observed (Fig. 6B; Inada et al. 1999; Kim et al. 1999). In the *Runx2*$^{-/-}$ tibiae as well as the wild-type tibiae at E18.5, BrdU-positive cells were restricted to the layers of resting and proliferating chondrocytes (Fig. 6A,B), whereas BrdU-positive cells were detected throughout the entire tibiae of *Runx2*$^{-/-}$*3*$^{+/-}$ and *Runx2*$^{-/-}$*3*$^{-/-}$ embryos (Fig. 6C,D). Further, in the *Runx2*$^{-/-}$*3*$^{-/-}$ tibiae, the BrdU-positive cells were distributed homogeneously and the columnar alignment of chondrocytes, which is formed by proliferation along a proximal–distal axis, was completely absent (Fig. 6D), indicating that the maturational blockage resulted in disorganized chondrocyte proliferation. In regions I and II, which represent the layers of resting and proliferating chondrocytes, respectively, in wild-type mice, *Runx2* deficiency, but not *Runx3* deficiency, significantly reduced chondrocyte proliferation (Fig. 6E). In region III, which represents the layers of hypertrophic and terminal hypertrophic chondrocytes in wild-type mice, there were no BrdU-positive cells in wild-type, *Runx3*$^{-/-}$, or *Runx2*$^{-/-}$ mice, whereas numbers of BrdU-positive cells similar to those in regions I and II were observed in *Runx2*$^{-/-}$*3*$^{+/-}$ and *Runx2*$^{-/-}$*3*$^{-/-}$ mice in the diaphyses (region III; Fig. 6E). In both tibiae and femurs, the decrease in proliferation was related to the *Runx2* deficiency but not to the *Runx3* deficiency in combined regions, which contained BrdU-positive cells (Fig. 6F). These findings indicate that the reduction in limb length of *Runx2*$^{-/-}$ mice was due to the reduced proliferation, demonstrating that Runx2 is involved in enhancing chondrocyte proliferation.

As the gene dosage of *Runx3* further affected the limb length in *Runx2*$^{-/-}$ mice, we examined the cell number, matrix area, and cell size in tibiae of *Runx2*$^{-/-}$, *Runx2*$^{-/-}$*3*$^{+/-}$, and *Runx2*$^{-/-}$*3*$^{-/-}$ mice. The cell number in each region was not significantly different among these mice, resulting in similar numbers of total cells in tibiae in these mice (Fig. 6G). Although the matrix area was similar among these mice (Fig. 6H), the cell size was reduced in region III in dependence on the gene dosage of *Runx3* (Fig. 6I). Further, the growth of the limbs to a longitudinal direction but not to a radial direction was disturbed in *Runx2*$^{-/-}$*3*$^{-/-}$ mice, leading to the further reduction in the limb length of *Runx2*$^{-/-}$*3*$^{-/-}$ mice. These findings indicate that the reduction in cell size in the diaphyses and the disorganized chondrocyte proliferation led to the severe reduction in the limb length of *Runx2*$^{-/-}$*3*$^{-/-}$ mice, and demonstrate that Runx2 and Runx3 play an important role in organizing chondrocyte proliferation in the limb skeletons to a longitudinal direction. However, apoptosis was not a major cause of the reduced limb length in *Runx2*$^{-/-}$*3*$^{+/-}$ and *Runx2*$^{-/-}$*3*$^{-/-}$ mice, because we detected TUNEL-positive cells in the terminal hypertrophic chondrocytes of *Runx2*$^{-/-}$ mice but not in the chondrocytes of *Runx2*$^{-/-}$*3*$^{+/-}$ or *Runx2*$^{-/-}$*3*$^{-/-}$ mice (data not shown).

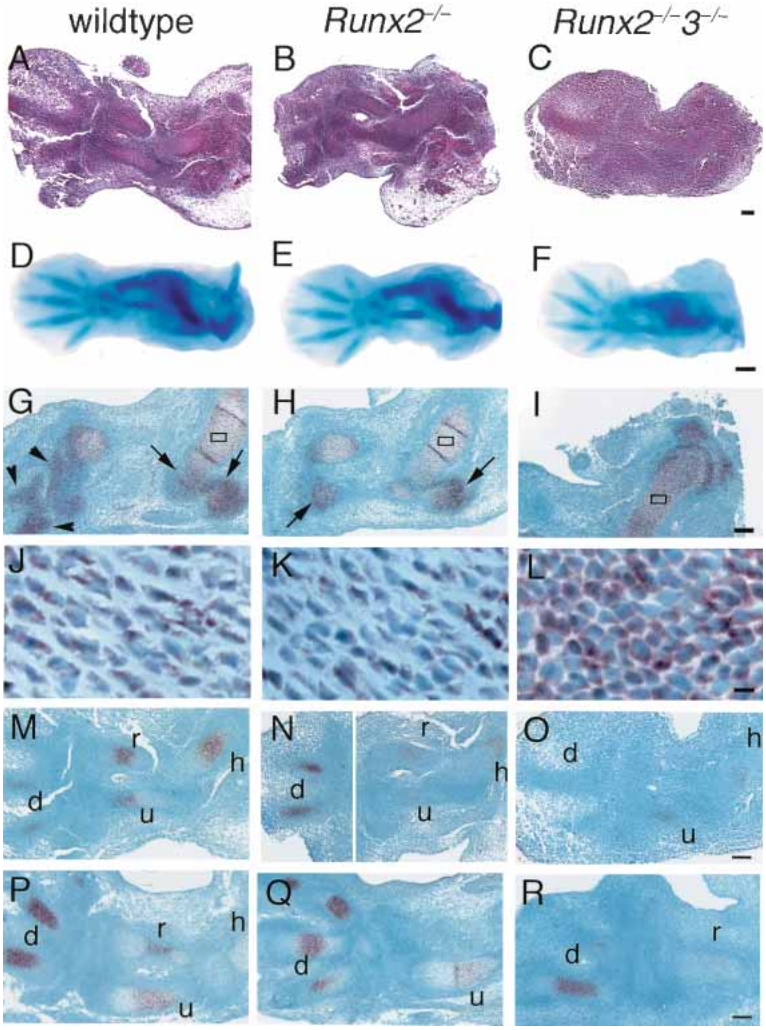

Figure 3. Early skeletal development in wild-type, *Runx2*$^{-/-}$, and *Runx2*$^{-/-}$*3*$^{-/-}$ embryos and in situ hybridization for *Sox9* and *Ihh* expression. We used the forelimbs (*A–C*,*G–R*) and hind limbs (*D–F*) of wild-type (*A*,*D*,*G*,*J*,*M*,*P*), *Runx2*$^{-/-}$ (*B*,*E*,*H*,*K*,*N*,*Q*), and *Runx2*$^{-/-}$*3*$^{-/-}$ (*C*,*F*,*I*,*L*,*O*,*R*) embryos for the analyses. (*A–C*) H&E staining at E12.5. (*D–F*) Whole-mount Alcian blue staining at E13.5. (*G–L*) In situ hybridization using *Sox9* antisense probe at E13.5. (*J–L*) Higher magnification of boxed regions in *G–I*, respectively. (*M–R*) In situ hybridization using *Ihh* antisense probe at E12.5 (*M–O*) and E13.5 (*P–*R). We detected no signal using the sense probe of *Sox9* and *Ihh* (data not shown). Cartilaginous anlagen was clearly seen in the wild-type (*A*) and *Runx2*$^{-/-}$ (*B*) embryos but not in the *Runx2*$^{-/-}$*3*$^{-/-}$ embryos (*C*) at E12.5. Alcian blue staining of the hind limbs of E13.5 *Runx2*$^{-/-}$*3*$^{-/-}$ embryos (*F*) was weak, compared with that of the wild-type (*D*) and *Runx2*$^{-/-}$ (*E*) embryos. (*G*,*H*,*J*,*K*) In the forelimb skeletons of wild-type and *Runx2*$^{-/-}$ embryos, the peripheral regions of the epiphyses of the humeri, radii, and ulnae (arrows in *G*,*H*), and most regions of the carpal and metacarpal bones (arrowheads in *G*) were composed of immature chondrocytes that strongly expressed *Sox9*, and the remaining regions of the humeri, radii, and ulnae, which were composed of differentiating chondrocytes, weakly expressed *Sox9*. (*I*,*L*) In the *Runx2*$^{-/-}$*3*$^{-/-}$ forelimb skeletons, all of the chondrocytes strongly expressed *Sox9*. *Ihh* was strongly detected in immature chondrocytes. especially in digits of wild-type, *Runx2*$^{-/-}$, and *Runx2*$^{-/-}$*3*$^{-/-}$ mice. (h) humerus; (r) radius; (u) ulna; (d) digit. Bars: *A–C*,*G–I*,*M–R*, 100 μm; *D–F*, 500 μm; *J–L*, 10 μm.

Regulation of Ihh *expression by Runx2 and Runx3*

In the present study, *Ihh* expression was reduced depending on the degree of maturational blockage of chondrocytes, and it was absent in *Runx2*$^{-/-}$*3*$^{-/-}$ skeletons (Figs. 5M–P; 7A). Thus, we next examined whether Runx2 and Runx3 directly regulate *Ihh* expression using *Runx2*$^{-/-}$ chondrocyte cultures (Fig. 7C–F). Adenoviral introduction of *Runx2* into *Runx2*$^{-/-}$ chondrocytes strongly induced *Ihh* expression at 6 h after the onset of infection, whereas the introduction of *Runx3* into *Runx2*$^{-/-}$ chondrocytes failed to induce *Ihh* expression (Fig. 7D). Introduction of *Runx2* or *Runx3* into *Runx2*$^{-/-}$ chondrocytes induced matrix metalloproteinase 13 (*Mmp13*) expression (Fig. 7E), which is a downstream gene of Runx2 (Inada et al. 1999; Jimenez et al. 1999), but did not up-regulate *Col10a1* expression (Fig. 7F). As *Runx2* and *Ihh* expression are both up-regulated in prehypertrophic chondrocytes (Bitgood and McMahon 1995; Vortkamp et al. 1996; Iwasaki et al. 1997; Zou et al. 1997; Inada et al. 1999; Kim et al. 1999), these findings suggest that Runx2 directly induces *Ihh* expression. As there was weak *Ihh* expression in *Runx2*$^{-/-}$ tibiae (Figs. 5N, 7A), this finding indicates that either Runx3 promotes *Ihh* expression indirectly or additional factors are required for *Ihh* induction by Runx3.

Regulation of the promoter of Ihh *by Runx2*

A database search revealed that the 1.2-kb promoter region of the *Ihh* gene was highly conserved between mouse and human (*Mus musculus* chromosome 1 genomic contig, NT_039170; *Homo sapiens* chromosome 2 genomic contig, NT_005403). The 1.2-kb promoter region of the mouse *Ihh* gene contained seven putative Runx binding sites (R1–R7), in which R1, R2, R4, R5, and R7 were conserved between mouse and human (Fig. 8A). The binding of Runx2 to the 1.2 kb *Ihh* promoter was confirmed by chromatin immunoprecipitation (ChIP; Fig. 8B). Four putative Runx binding sites (R1, R2, R4, and R5) had perfectly corresponding sequences with the binding sequences of Runx, and Runx2 strongly bound to each of the four oligonucleotides in the electrophoresis mobility shift assay (EMSA; Fig. 8C). The other putative Runx binding sites (R3, R6, and R7) included one less

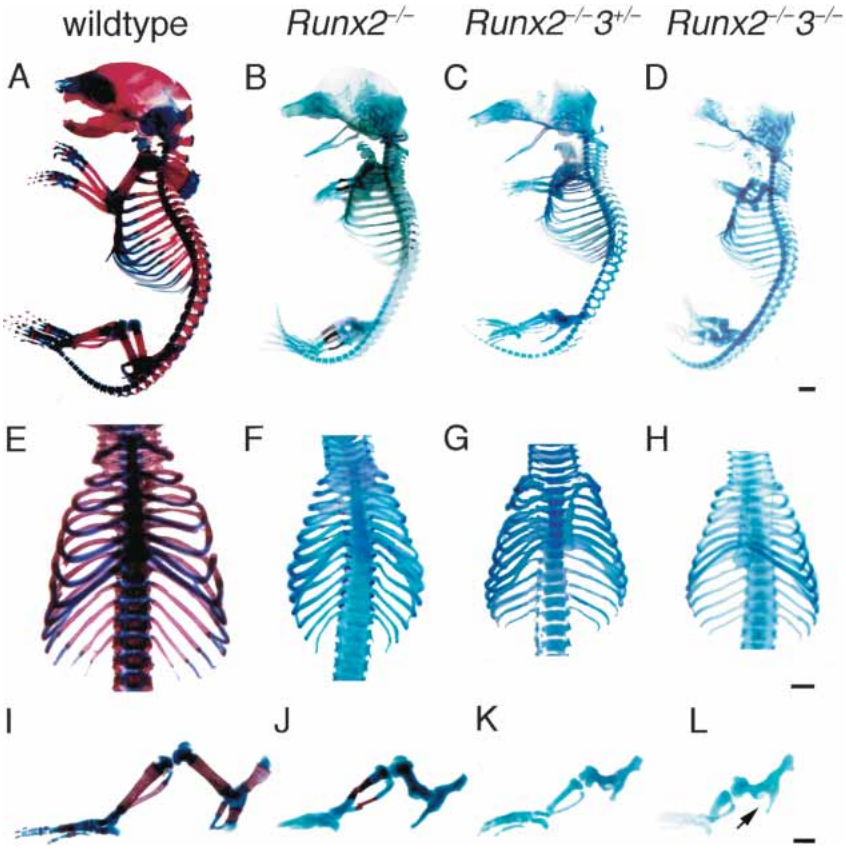

Figure 4. Examination of the skeletal system of wild-type, *Runx2*$^{-/-}$, *Runx2*$^{-/-}$*3*$^{+/-}$, and *Runx2*$^{-/-}$*3*$^{-/-}$ mice at the newborn stage. Skeletons of wild-type (*A*,*E*,*I*), *Runx2*$^{-/-}$ (*B*,*F*,*J*), *Runx2*$^{-/-}$*3*$^{+/-}$ (*C*,*G*,*K*), and *Runx2*$^{-/-}$*3*$^{-/-}$ (*D*,*H*,*L*) newborns. (*A–D*) Whole skeletons. (*E–H*) Chest walls. (*I–L*) Hind limbs. Although mineralization was observed in restricted skeletal parts including the limbs, vertebrae, and ribs of *Runx2*$^{-/-}$ mice (*B*,*F*,*J*), it was completely absent in *Runx2*$^{-/-}$*3*$^{+/-}$ (*C*,*G*,*K*) and *Runx2*$^{-/-}$*3*$^{-/-}$ mice (*D*,*H*,*L*). Note that the limb length was reduced depending on the dosages of *Runx2* and *Runx3*, and that *Runx2*$^{-/-}$*3*$^{-/-}$ mice have severely shortened but relatively thick limbs (*I–L*). *Runx2*$^{-/-}$*3*$^{-/-}$ mice completely lack a pubic bone structure (arrow in *L*). Bars: *A–L*, 1 mm.

common base, and Runx2 bound relatively strongly to the R7 oligonucleotides and weakly to the R3 and R6 oligonucleotides. Competition assays also showed that Runx2 bound strongly to the R1, R2, R4, and R5 oligonucleotides, to the R7 oligonucleotides less strongly, but to the R3 and R6 oligonucleotides barely (Fig. 8D). Further, reporter assays of various deletion constructs of the 1.2-kb promoter region of the *Ihh* gene using *Runx2*$^{-/-}$ chondrocytes and chondrogenic ATDC5 cells showed that Runx2 strongly activated the *Ihh* promoter, and that R1, R5, and R7 are important Runx2 binding sites for transcriptional activation (Fig. 8E). As the reporter activity was significantly reduced in the p1112-luc construct, inhibitory factors seem to bind around R6 in the *Ihh* promoter region. In contrast to Runx2, Runx3 failed to activate the 1.3-kb *Ihh* promoter, although Runx3 bound to the R2 oligonucleotides (Fig. 8F,G).

Discussion

We demonstrated here that chondrocyte maturation is dependent on the dosages of *Runx2* and *Runx3*, and that the absence of both *Runx2* and *Runx3* causes a complete lack of chondrocyte maturation. We further showed that Runx2 enhances chondrocyte proliferation through the direct induction of *Ihh* expression. Thus, Runx2 and Runx3 play fundamental roles in skeletal development by regulating and coordinating chondrocyte maturation and proliferation to form endochondral bones of appropriate size and shape.

The degree of the disturbance of chondrocyte maturation in *Runx2*$^{-/-}$ mice depended on the skeletal part (Inada et al. 1999; Kim et al. 1999), whereas the chondrocytes in all skeletal parts of *Runx2*$^{-/-}$*3*$^{-/-}$ mice failed to mature (Figs. 5, 6; data not shown). This indicates that the level of *Runx3* expression or Runx3 activation differs in different parts of the skeleton, because the deficiency of *Runx2* has no significant effect on the expression level of *Runx3* (Stricker et al. 2002). Indeed, Runx2 plays a larger role in promoting chondrocyte maturation than Runx3, because chondrocyte maturation was more delayed in *Runx2*$^{-/-}$ mice than in *Runx3*$^{-/-}$ mice in all skeletal parts (Figs. 2, 5; data not shown). Although Sox9, which is an inhibitor of chondrocyte maturation (Akiyama et al. 2002), was strongly expressed in E13.5 *Runx2*$^{-/-}$*3*$^{-/-}$ cartilage (Fig. 3I,L), its expression decreased during development, indicating that the chondrocytes in *Runx2*$^{-/-}$*3*$^{-/-}$ cartilage were released from the inhibitory effect of Sox9 on maturation. However, the chondrocytes in *Runx2*$^{-/-}$*3*$^{-/-}$ cartilage failed to mature, as shown by the homogeneously small chondrocytes and the absence of expression of all of the chondrocyte maturation marker genes, including *Pthr1*, *Ihh*, and *Col10a1*, at E18.5 (Figs. 5, 6A–D, 7A,B), demonstrating that Runx2 and Runx3 are essential transcription factors for chondrocyte maturation.

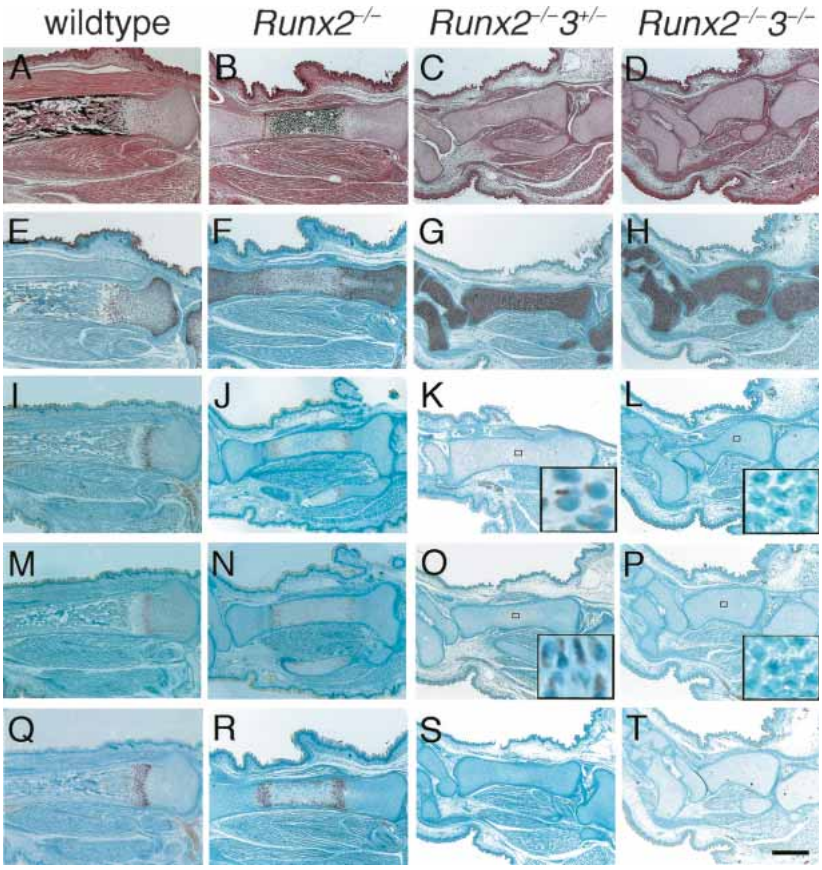

Figure 5. Histological examination and in situ hybridization for *Col2a1*, *Pthr1*, *Ihh*, and *Col10a1* in the tibiae of wild-type, *Runx2*$^{-/-}$, *Runx2*$^{-/-}$*3*$^{+/-}$, and *Runx2*$^{-/-}$*3*$^{-/-}$ embryos at E18.5. Sections of tibiae from wild-type (*A*,*E*,*I*,*M*,*Q*), *Runx2*$^{-/-}$ (*B*,*F*,*J*,*N*,*R*), *Runx2*$^{-/-}$*3*$^{+/-}$ (*C*,*G*,*K*,*O*,*S*), and *Runx2*$^{-/-}$*3*$^{-/-}$ (*D*,*H*,*L*,*P*,*T*) embryos were examined by H&E and Kossa staining (*A–D*) and in situ hybridization using the antisense probes of *Col2a1* (*E–H*), *Pthr1* (*I–L*), *Ihh* (*M–P*), or *Col10a1* (*Q–T*). The boxed regions in *K*, *L*, *O*, and *P* are magnified in the respective *insets*. On in situ hybridization of *Pthr1* and *Ihh*, signal detection using the sections from *Runx2*$^{-/-}$ and *Runx2*$^{-/-}$*3*$^{+/-}$ tibiae always took a longer period of time than that using sections from wild-type tibiae. Further, we failed to detect *Pthr1* and *Ihh* expression in *Runx2*$^{-/-}$*3*$^{-/-}$ tibiae even upon prolonged incubation. We detected no signal using sense probes of *Col2a1*, *Pthr1*, *Ihh*, and *Col10a1* (data not shown). In the tibiae of wild-type embryos, the cartilage was largely replaced by bone, whereas all of the *Runx2*$^{-/-}$, *Runx2*$^{-/-}$*3*$^{+/-}$, and *Runx2*$^{-/-}$*3*$^{-/-}$ tibiae were cartilaginous. In the *Runx2*$^{-/-}$ tibiae, the diaphyses were composed of calcified cartilage and chondrocytes in the metaphyses expressed *Pthr1*, *Ihh*, or *Col10a1*. In contrast, *Runx2*$^{-/-}$*3*$^{+/-}$ and *Runx2*$^{-/-}$*3*$^{-/-}$ tibiae showed no mineralization and the chondrocytes in the entire tibiae expressed *Col2a1* but not *Col10a1*. *Pthr1* and *Ihh* expression were very weakly detected in the diaphyses of *Runx2*$^{-/-}$*3*$^{+/-}$ tibiae, but they were not detected in *Runx2*$^{-/-}$*3*$^{-/-}$ tibiae (see *insets* in *K*,*L*,*O*,*P*). Bar, 500 μm.

The Runx family consists of three genes, *Runx1*, *Runx2*, and *Runx3* (Komori 2002). *Runx1*$^{-/-}$ mice die at approximately E12.5 due to the absence of fetal liver hematopoiesis, demonstrating that Runx1 is essential for definitive hematopoiesis (Okuda et al. 1996; Wang et al. 1996; Okada et al. 1998). As Runx1 was also expressed in cartilage (Levanon et al. 2001), we generated *Runx1*$^{+/-}$*2*$^{-/-}$ mice and examined their skeletal development. The degree of maturational delay of the chondrocytes in *Runx1*$^{+/-}$*2*$^{-/-}$ mice was the same as that in *Runx2*$^{-/-}$ mice (C. Yoshida and T. Komori, unpubl.), whereas the maturational delay of the chondrocytes in *Runx2*$^{-/-}$*3*$^{+/-}$ mice was more severe than that in *Runx2*$^{-/-}$ mice (Fig. 5), indicating that the contribution of Runx1 in chondrocyte maturation, if any, seems to be limited.

Expression of a dominant negative form of Runx2 blocked maturation but increased the proliferation of cultured chick primary chondrocytes (Enomoto-Iwamoto et al. 2001). However, chondrocyte proliferation was reduced in *Runx2*$^{-/-}$ mice (Fig. 6), suggesting that regulatory factors that are induced during maturation promote chondrocyte proliferation in vivo. Ihh is the most plausible factor based on the following results: chondrocyte proliferation was reduced in *Ihh*$^{-/-}$ mice (St-Jacques et al. 1999); addition of Sonic hedgehog (Shh) and bone morphogenetic protein (BMP)-2 synergistically promoted the proliferation of cultured primary chondrocytes (Takamoto et al. 2003); and *Ihh* expression is upregulated during chondrocyte maturation (Bitgood and McMahon 1995; Vortkamp et al. 1996; Iwasaki et al. 1997; Zou et al. 1997). Although *Ihh* expression was detected in immature chondrocytes in *Runx2*$^{-/-}$ and *Runx2*$^{-/-}$*3*$^{-/-}$ mice as well as wild-type mice at E12.5 and E13.5 (Fig. 3M–R), *Ihh* expression in chondrocytes was reduced in *Runx2*$^{-/-}$ mice and was undetectable in *Runx2*$^{-/-}$*3*$^{-/-}$ mice at E18.5 (Figs. 5N,P, 7A). Therefore, it must be clarified whether the reduction in *Ihh* expression was a result of maturational blockage of chondrocytes or whether Runx2 and Runx3 are directly involved in *Ihh* expression. In the present study, Runx2 strongly induced *Ihh* expression shortly after adenoviral introduction of *Runx2* in *Runx2*$^{-/-}$ chondrocyte cultures (Fig. 7D). Further, the 1.2-kb promoter region of the mouse *Ihh* gene contained seven putative Runx binding sites, five of which were conserved in human, and Runx2 bound to the five Runx binding sites, thereby activating the promoter (Fig. 8A–E). These findings demonstrate that Runx2 directly regulates *Ihh* expression during chondrocyte maturation, but that neither Runx2 nor Runx3 is essential for the *Ihh* expression in the immature chondrocytes at the early stage of skeletal develop-

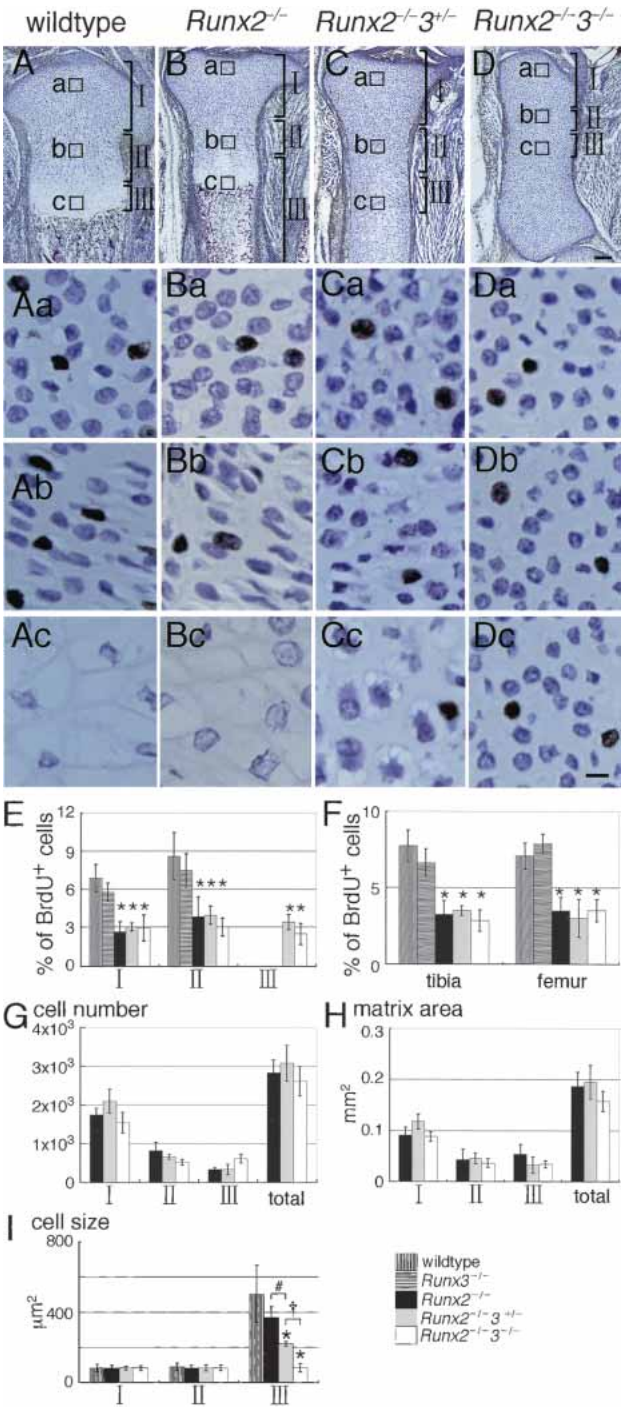

Figure 6. Analysis of chondrocyte proliferation in the limbs by BrdU labeling. (*A–D*) Immunohistochemistry of tibiae from BrdU-labeled wild-type (*A*), *Runx2*$^{-/-}$ (*B*), *Runx2*$^{-/-}$*3*$^{+/-}$ (*C*), and *Runx2*$^{-/-}$*3*$^{-/-}$ (*D*) embryos at E18.5 using anti-BrdU antibody. The sections were counterstained with toluidine blue. Magnified views of the boxed regions (*a*,*b*,*c*) are shown in the same columns. (*A*,*B*) In wild-type and *Runx2*$^{-/-}$ tibiae, the boxed regions *a*, *b*, and *c* represent resting, proliferating, and hypertrophic chondrocytes, respectively. (*C*,*D*) In the *Runx2*$^{-/-}$*3*$^{+/-}$ and *Runx2*$^{-/-}$*3*$^{-/-}$ tibiae, the boxed regions *a*, *b*, and *c* represent chondrocytes in the epiphyses, metaphyses, and diaphyses, respectively. The growth plates were well formed in wild-type tibiae (*A*) and in *Runx2*$^{-/-}$ tibiae (*B*) but not in *Runx2*$^{-/-}$*3*$^{+/-}$ tibiae (*C*) or *Runx2*$^{-/-}$*3*$^{-/-}$ tibiae (*D*). (*Ab–Db*) The columnar alignment of chondrocytes, which is seen in the layer of proliferating chondrocytes, is well formed in the wild-type and *Runx2*$^{-/-}$ tibiae, deformed in the *Runx2*$^{-/-}$*3*$^{+/-}$ tibiae, and completely absent in the *Runx2*$^{-/-}$*3*$^{-/-}$ tibiae. (*C*,*D*) The diaphyses of *Runx2*$^{-/-}$*3*$^{+/-}$ tibiae were composed of slightly enlarged chondrocytes, whereas the entire tibiae of *Runx2*$^{-/-}$*3*$^{-/-}$ embryos were composed of homogeneously small chondrocytes. (*E–I*) Measurement of the frequency of BrdU-positive cells (*E*,*F*), cell number (*G*), matrix area (*H*), and cell size (*I*) using the tibiae of six wild-type embryos, two *Runx3*$^{-/-}$ embryos, six *Runx2*$^{-/-}$ embryos, one *Runx2*$^{-/-}$*3*$^{+/-}$ embryo, and two *Runx2*$^{-/-}$*3*$^{-/-}$ embryos. We measured these parameters in each region shown in *A–D*. (*A*,*B*) In wild-type and *Runx2*$^{-/-}$ tibiae, the regions I, II, and III represent resting, proliferating, and hypertrophic and terminal hypertrophic chondrocytes, respectively. (*C*,*D*) In the *Runx2*$^{-/-}$*3*$^{+/-}$ and *Runx2*$^{-/-}$*3*$^{-/-}$ tibiae, the regions I, II, and III were arbitrarily determined in the proximal half of the tibiae and represent chondrocytes in the epiphysial, metaphysical, and diaphysial parts of the tibiae, respectively. (*F*) We also counted the number of BrdU-positive cells in femurs, because chondrocyte maturation in *Runx2*$^{-/-}$ femurs is more severely inhibited than that in *Runx2*$^{-/-}$ tibiae (Inada et al. 1999). (*F*) In the measurement of BrdU-positive cells in whole tibiae and femurs, we counted the number of BrdU-positive cells and the total number of cells in regions I and II in wild-type and *Runx2*$^{-/-}$ mice and in regions I, II, and III in *Runx2*$^{-/-}$*3*$^{+/-}$ and *Runx2*$^{-/-}$*3*$^{-/-}$ mice, and the mean of the percentage of BrdU-positive cells ± standard deviation (std. dev.) is shown. We measured all of the parameters in three sections of each bone, and the mean ± std. dev. is shown. (*) $p < 0.0001$ compared with wild-type mice; (#) $p < 0.0001$; (†) $p < 0.0001$ as determined by one-way ANOVA. Bars: *A–D*, 100 μm; *Aa–Dc*, 10 μm.

ment. Thus, our findings indicate that Runx2 enhances chondrocyte proliferation through the induction of *Ihh* expression during chondrocyte maturation. Interestingly, Shh induced *Runx2* expression and activated the *Runx2* promoter in primary chondrocyte cultures (Takamoto et al. 2003). Therefore, there may be a positive feedback loop between Ihh and Runx2. In contrast, Runx3 failed to induce *Ihh* expression in *Runx2*$^{-/-}$ chondrocyte cultures (Fig. 7D), and it failed to activate the *Ihh* promoter (Fig. 8G). Therefore, either the induction of *Ihh* by Runx3 is indirect or other factors are required for the induction of *Ihh* expression. We examined the requirement of soluble factors in Runx3-dependent *Ihh* expression. However, the addition of BMP-7, transforming growth factor-β (TGF-β), retinoic acid, insulin-like growth factor 1 (IGF-1), basic fibroblast growth factor (bFGF), platelet-derived growth factor (PDGF), parathyroid hormone (PTH), or T3 to *Runx3*-overexpressing *Runx2*$^{-/-}$ chondrocyte cultures failed to induce *Ihh* expression, although BMP-2 had a mild effect on *Ihh* ex-

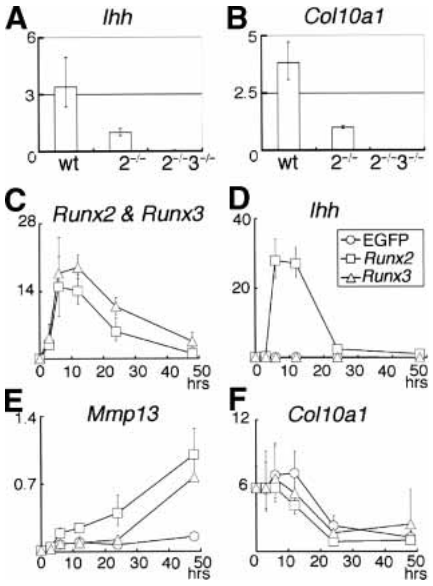

Figure 7. Regulation of *Ihh* expression by Runx2 and Runx3. (*A*,*B*) Real-time RT–PCR analysis of *Ihh* (*A*) and *Col10a1* (*B*) expression using RNA extracted from wild-type (wt), *Runx2*$^{-/-}$ (2$^{-/-}$), and *Runx2*$^{-/-}$*3*$^{-/-}$ (2$^{-/-}$3$^{-/-}$) limbs at E18.5. The mean of two to three embryos is shown. The values in *Runx2*$^{-/-}$ limbs were defined as 1, and relative values are shown. (*C–F*) Real-time RT–PCR analysis of *Runx2*$^{-/-}$ chondrocyte cultures. *Runx2*$^{-/-}$ chondrocytes were infected with EGFP-expressing (○), *Runx2*-and-EGFP-expressing (□), or *Runx3*-and-EGFP-expressing (△) adenovirus. Infected cells were harvested at the indicated times after the onset of viral infection, and *Runx2* (*C*), *Runx3* (*C*), *Ihh* (*D*), *Mmp13* (*E*), and *Col10a1* (*F*) expression were examined by real-time RT–PCR. The value of *Runx2* mRNA expression at 48 h was defined as 1, and the relative values of *Runx2* and *Runx3* mRNA expression are shown in the same graph (*Runx2* and *Runx3*). In the cells infected with EGFP-expressing adenovirus, the values of *Runx2* mRNA expression were nearly zero and the values of *Runx3* mRNA expression were very low; therefore, they were not included in the graph. The value of *Ihh*, *Mmp13*, or *Col10a1* mRNA expression in *Runx2*-and-EGFP-expressing adenovirus infection at 48 h was defined as 1, and relative values are shown. Adenoviral introduction of *Runx2* strongly up-regulated *Ihh* expression, whereas adenoviral introduction of *Runx3* did not up-regulate *Ihh* expression. In the cells infected with any of the three adenoviruses, the level of *Col10a1* expression was at the background level during the culture period examined. Data represent the mean of three to six wells, and representative data of three independent experiments are shown.

pression irrespective of the *Runx3* overexpression (data not shown).

Ihh was weakly expressed in *Runx2*$^{-/-}$ cartilage but not at all in *Runx2*$^{-/-}$*3*$^{-/-}$ cartilage (Figs. 5N,P, 7A). However, the absence of *Ihh* expression in *Runx2*$^{-/-}$*3*$^{-/-}$ cartilage did not result in further reduction in the chondrocyte proliferation, indicating that there was no complete correlation between the degree of inhibition of proliferation and the level of *Ihh* expression (Fig. 6E,F). As immature chondrocytes have more capacity for proliferation than mature chondrocytes in vitro (Enomoto et al. 2000; Enomoto-Iwamoto et al. 2001), the severe inhibition of chondrocyte maturation in *Runx2*$^{-/-}$*3*$^{+/-}$ and *Runx2*$^{-/-}$*3*$^{-/-}$ mice may have enhanced the chondrocyte proliferation in an Ihh-independent manner and compensated for the reduction in proliferation due to the reduced *Ihh* expression. However, Ihh, even at a low dose mediated by Runx3, may play an important role in organizing chondrocyte proliferation to a longitudinal direction, because the loss of columnar alignment of chondrocytes was well correlated with the disappearance of *Ihh* expression (Figs. 5N–P, 6B–D).

As the addition of Pthlh inhibited Runx2-induced maturation of cultured chick primary chondrocytes (Iwamoto et al. 2003), up-regulation of *Ihh* expression by Runx2 is also important as a negative feedback pathway through Pthlh to acquire an appropriate rate of chondrocyte maturation. Thus, in addition to the essential role of Runx2 and Runx3 in chondrocyte maturation, Runx2 is involved in coordinating the maturation and proliferation of chondrocytes, which is required for the formation of skeletal parts of appropriate size and shape, through the regulation of *Ihh* expression.

Materials and methods

Generation of Runx2$^{-/-}$*3*$^{-/-}$ *mice*

We generated *Runx2*$^{+/-}$ mice and *Runx3*$^{+/-}$ mice as described (Komori et al. 1997; Li et al. 2002). We mated *Runx2*$^{+/-}$ mice with *Runx3*$^{+/-}$ mice to generate *Runx2*$^{+/-}$*3*$^{+/-}$ mice. We further mated *Runx2*$^{+/-}$*3*$^{+/-}$ males with *Runx2*$^{+/-}$*3*$^{+/-}$ females to generate *Runx2*$^{-/-}$*3*$^{-/-}$ mice. We determined each genotype of *Runx2* and *Runx3* by PCR using tail DNA using the following primers: *Runx2*, 5′-AGCTTTAGCGTCGTCAGACC-3′ and 5′-CAGGTTCAGCAGTCCATCTC-3′, 5′-AGCTTTAGCGTCGTCAGACC-3′ and 5′-CAAGCGAAACATCGCATCGAGC-3′; *Runx3*, 5′-GACTGTGCATGCACCTTTCACCAA-3′ and 5′-TAGGGCTCAGTAGCACTTACGTCG-3′, 5′-GACTGTGCATGCACCTTTCACCAA-3′ and 5′-ATGAAACGCCGAGTTAACGCCATCA-3′. Prior to the study, all experiments were reviewed and approved by the Osaka University Medical School Animal Care and Use Committee.

Detection of β*-galactosidase activity, skeletal preparation, and analyses of histology, BrdU incorporation, and matrix and cell parameters*

To study the localization of *Runx3* expression, we examined the activity of β-galactosidase, whose gene was integrated in exon 3 of *Runx3* in *Runx3*$^{+/-}$ mice (Li et al. 2002) as described (Ueta et al. 2001). We embedded stained embryos in paraffin and generated 7-μm sections. Newborn skeletons were stained with Alcian blue and Alizarin red as described (Komori et al. 1997). For histological analysis, we fixed embryos in 4% paraformaldehyde, embedded them in paraffin, and prepared 7-μm sections to perform hematoxylin and eosin (H&E) staining, double staining with H&E and von Kossa, or Alcian blue staining as described (Ueta et al. 2001). For analysis of BrdU incorporation, we intraperitoneally injected pregnant mice with 50 μg BrdU/g body weight 1 h before sacrifice. We processed the embryos for histological analysis and detected BrdU incorporation by immunohistochemistry using anti-BrdU antibody (Dako). We counterstained the sections with toluidine blue. For the analyses of

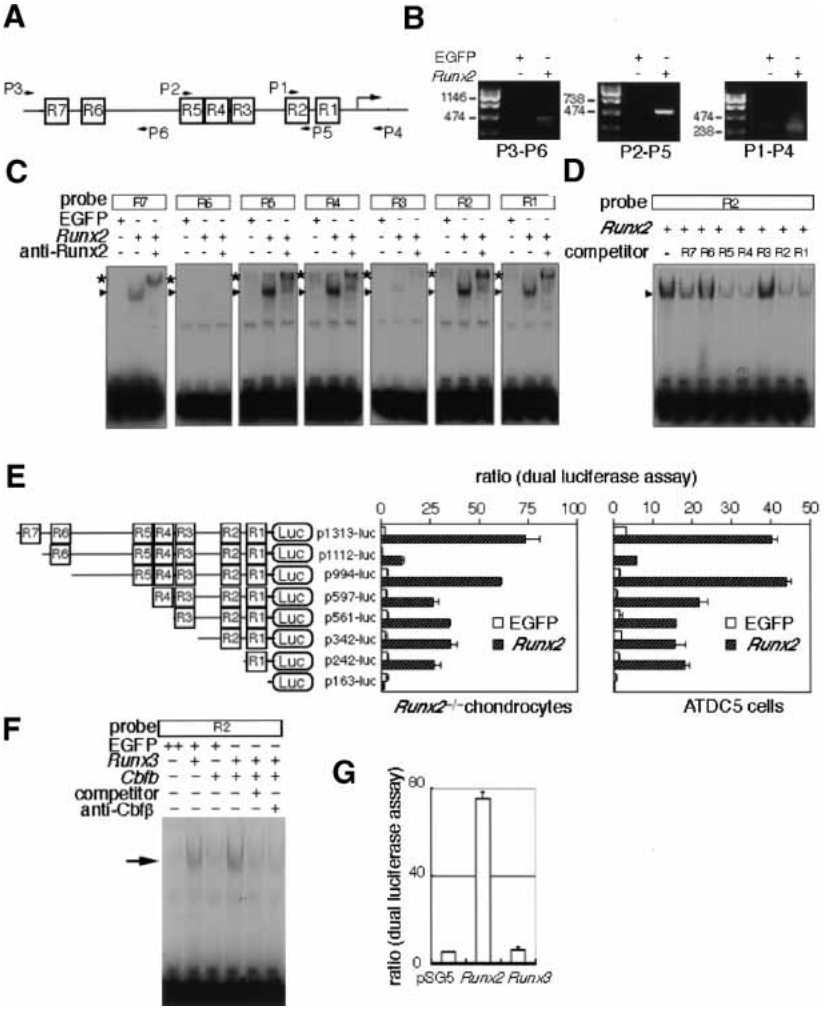

Figure 8. Regulation of the *Ihh* promoter by Runx2. (*A*) Schematic presentation of seven putative Runx-binding sites (R1–R7) and primers used for ChIP in the promoter region of the mouse *Ihh* gene. (*B*) ChIP. *Runx2*$^{-/-}$ chondrocytes were infected with EGFP- or *Runx2*-and-EGFP-expressing adenovirus. After sonication, the cell lysates were immunoprecipitated by anti-Runx2 antibody, and the binding of Runx2 to the *Ihh* promoter region was examined by PCR using the primers shown in *A*. Bands of correct sizes were detected in *Runx2*-expressing cells, and the amplified DNA contained each *Ihh* promoter fragment, which was confirmed by sequencing (data not shown). (*C*) Binding of Runx2 to the putative Runx binding sequences. *Runx2*$^{-/-}$ chondrocytes were infected with EGFP- or *Runx2*-and-EGFP- expressing adenovirus, and EMSA was performed using each of the R1–R7 probes. Runx2 strongly bound to R1, R2, R4, and R5, less strongly to R7, and weakly to R3 and R6. All of the specific bands (arrowheads) were supershifted with anti-Runx2 antibody (*). All of the specific bands were competed with the respective unlabeled oligonucleotide (data not shown). (*D*) The affinity of Runx2 for each putative Runx binding sequence. *Runx2*$^{-/-}$ chondrocytes were infected with *Runx2*-and-EGFP-expressing adenovirus, and EMSA was performed using labeled R2 probe in the presence of each unlabeled oligonucleotide (R1–R7/×200). The formation of the Runx2–R2 complex was strongly inhibited in the presence of unlabeled R1, R2, R4, or R5 oligonucleotides, less strongly inhibited in the presence of unlabeled R7 oligonucleotides, but barely inhibited in the presence of unlabeled R3 or R6 oligonucleotides. (*E*) Reporter assays of the *Ihh* promoter. The reporter plasmid containing each *Ihh* promoter construct and pRL-CMV vector were cotransfected into *Runx2*$^{-/-}$ chondrocytes (*left*) or ATDC5 cells (*right*). After culture for 24 h, Runx2 was adenovirally introduced into the cells at an MOI of 10. The data show the relative level of luciferase activity against the level of *Renilla* luciferase activity. The values are mean ± S.E. of four wells, and representative data from four independent experiments are shown. (*F*) Binding of Runx3 to the R2 oligonucleotides. *Runx2*$^{-/-}$ chondrocytes were infected with retrovirus expressing EGFP alone or *Cbfb* and EGFP. After 1 d, the cells were infected with EGFP- or *Runx3*-and-EGFP-expressing adenovirus, and EMSA was performed using the R2 probe. The introduction of *Runx3* alone showed a specific band (arrow), and the intensity of the specific band was increased by the introduction of *Cbfb*. The specific band was competed with unlabeled R2 oligonucleotides (×200). Addition of antibody against Cbfβ prevented formation of the specific Runx3–Cbfβ–DNA complexes. (*G*) Reporter assay using the 1.3-kb *Ihh* promoter. To compare the capacities of Runx2 and Runx3 in the transcriptional activation of *Ihh* promoter, *Runx2*$^{-/-}$ chondrocytes were transiently transfected with DNA mixture containing p1313-luc, *Runx2*- or *Runx3*-expressing vector or empty pSG5, and pRL-CMV. The luciferase activity was normalized to *Renilla* luciferase activity.

matrix and cell parameters, we prepared 4-μm sections and stained the sections with safranin O. The cell number, area of matrix, and cell size were analyzed using Mac Scope 2.6 software (Mitani).

In situ hybridization

For in situ hybridization, we prepared digoxigenin-11-UTP-labeled single-stranded RNA probes using a DIG RNA labeling kit (Roche Biochemica) according to the manufacturer's instructions. We used a 0.4-kb fragment of *Col2a1* cDNA (Inada et al. 1999), a 0.65-kb fragment of mouse *Col10a1* cDNA (Inada et al. 1999), a 1.2-kb fragment of osteopontin cDNA (Komori et al. 1997), a 0.4-kb fragment of mouse *Sox9* cDNA (nt 723–1263, NM-011448), a 0.8-kb fragment of mouse *Pthr1* cDNA (Inada et al. 1999), and a 0.6-kb fragment of mouse *Ihh* cDNA (Inada et al. 1999) to generate antisense and sense probes. We carried out hybridization as described previously and counterstained the sections with methyl green.

Cell culture and adenoviral transfer

We isolated chondrocytes from the skeletons of E18.5 *Runx2*$^{-/-}$ embryos, plated them at a density of 1×10^5 cells/well in 24-well plates (Corning), and cultured them in DMEM/Ham's F12 (1:1) hybrid medium (GIBCO-BRL) containing 10% fetal bovine serum (FBS; GIBCO-BRL) as described (Enomoto et al. 2004). When the cells reached confluence, we infected the cells with

enhanced green fluorescent protein (EGFP)-expressing adenovirus, *Runx2*-and-EGFP-expressing adenovirus, or *Runx3*-and-EGFP-expressing adenovirus for 2 h at a multiplicity of infection (MOI) of 10 in 0.2 mL medium. After the medium was added up to 1 mL, the cells were cultured for 46 h. The infected cells were harvested for real-time RT–PCR at the indicated times after the onset of viral infection. We generated bicistronic adenovirus vectors expressing *Runx2* and EGFP or EGFP alone as described (Enomoto et al. 2003). We generated a bicistronic adenovirus vector expressing *Runx3* and EGFP using human *Runx3* cDNA (Bae et al. 1995).

Real-time RT–PCR

Total RNA that had been extracted from wild-type, *Runx2*$^{-/-}$, and *Runx2*$^{-/-}$*3*$^{-/-}$ limb skeletons at E18.5 and *Runx2*$^{-/-}$ chondrocytes was reverse transcribed using M-MLV reverse transcriptase. We mixed the cDNA (7.5 ng total RNA equivalent) with SYBR Green PCR Master Mix (Applied Biosystems) and analyzed it by real-time PCR using the ABI7700 (Applied Biosystems). Primers used for amplification were as follows: *Ihh*, 5′-TTCAAGGACGAGGAGAACACG-3′ and 5′-TTCAGACG GTCCTTGCAGC-3′; *Col10a1*, 5′-AGAACGGCACGCCTAC GAT-3′ and 5′-AGGTAGCCTTTGCTGTACTCATCAT-3′; *Runx2*, 5′-CCGCACGACAACCGCACCAT-3′ and 5′-CGCTC CGGCCCACAAATCTC-3′; *Runx3*, 5′-GGTTCAACGACCTT CGCTTC-3′ and 5′-CACGGTCACCTTGATGGCT-3′; *Mmp13*, 5′-TCACCTGATTCTTGCGTGCT-3′ and 5′-CTGTGGGTT ATTATCAATCTTGTTTCTT-3′. We normalized the obtained CT (cycle number at which amplification threshold of detection was reached) values for *Ihh*, *Col10a1*, *Runx2*, *Runx3*, and *Mmp13* to that of rodent *Gapdh* (Applied Biosystems) expression by the ΔΔCT method. The mean ΔΔCT was converted to relative expression value by the equation $2^{-\Delta\Delta Ct}$, and the range was calculated by the equation $2^{-(\Delta\Delta Ct + StdevdeltaCt)}$.

ChIP

Chondrocytes from *Runx2*$^{-/-}$ embryos at E18.5 were infected with EGFP- or *Runx2*-and-EGFP-expressing adenovirus at an MOI of 10. ChIP was performed as described (Takahashi et al. 2000). After immunoprecipitation using monoclonal anti-Runx2 antibody (Yoshida et al. 2002) and DNA extraction, PCR was performed using the following primers in the promoter region of the mouse *Ihh* gene: P1, 5′-ATGGATAGGGTGCG GTCTGC-3′; P2, 5′-CTGAGAAAGGGAATGTTGCC-3′; P3, 5′-GTGAGGGTGAGGGAGGAAGA-3′; P4, 5′-GCGTGCTGT CCCCCTCGGCG-3′; P5, 5′-AGAGGGGAAATGGAAGAGAT-3′; P6, 5′-TAGGGGATGCGGGTGGAGGC-3′.

EMSA

We prepared nuclear extracts from chondrocytes of *Runx2*$^{-/-}$ embryos at E18.5 as described (Yoshida et al. 2002). Briefly, *Runx2*$^{-/-}$ chondrocytes were infected with EGFP- or *Runx2*-and-EGFP- expressing adenovirus at an MOI of 10, and nuclear extracts were prepared 24 h later. The nuclear extracts were incubated with 10 fmol of each of ^{32}P-labeled double-stranded R1–R7 oligonucleotides, and EMSA was performed as described (Yoshida et al. 2002). The oligonucleotide sequences of R1–R7 were as follows: R1, 5′-GGATCCGCTAACCGCGGGTGGAT CC-3′; R2, 5′-GGATCCGGGTGCGGTCTGCGGATCC-3′; R3, 5′-GGATCCAGGA GCCGCAAGGGGATCC-3′; R4, 5′-GGAT CCGGTTGCGGTCTCCGGATCC-3′; R5, 5′-GGATCCTTGT GCGGTCCGGGGATCC-3′; R6, 5′-GGATCCGTCCG TGGC TTCTGGATCC-3′; R7, 5′-GGATCCCATTGTGGTGGTGGA TCC-3′. For supershift experiments, the monoclonal antibody against Runx2 (Yoshida et al. 2002) was added to the entire mixture. We carried out a competition with 200-fold molar excess of each unlabeled oligonucleotide of R1–R7. In the analysis of DNA binding of Runx3, *Runx2*$^{-/-}$ chondrocytes were infected with retrovirus expressing *Cbfb* and EGFP or EGFP alone by the bicistronic retroviral expression vector (Yoshida et al. 2002). After 1 d, the cells were infected with EGFP- or *Runx3*-and-EGFP- expressing adenovirus at an MOI of 10, and nuclear extracts were prepared 24 h later. For supershift experiments, the polyclonal antibody against Cbfβ (Yoshida et al. 2002) was added to the entire mixture.

Reporter assay

The 1.3-kb promoter region (–1208/+105) of the mouse *Ihh* gene was amplified by PCR using liver DNA from C57BL/6 × C3H F1. Various lengths of *Ihh* promoter fragments were generated either by restriction digests of the 1.3-kb *Ihh* promoter region or by PCR, and they were inserted into the pGL3 vector. All of the constructs were confirmed by sequencing. Chondrocytes from *Runx2*$^{-/-}$ embryos at E18.5 or ATDC5 cells in 48-well multiplates were transiently transfected with a DNA mixture containing each *Ihh* promoter construct (0.2 μg) and pRL-CMV (0.002 μg) using FuGENE 6 (Roche Diagnostics). After culture for 24 h, the cells were infected with EGFP- or *Runx2*-and-EGFP-expressing adenovirus at an MOI of 10. After 24 h, we assayed the luciferase activity of the cell lysate using the Dual Luciferase Reporter Assay System (Promega) and a model TD20/20 luminometer (Promega). The level of luciferase activity was normalized to the level of *Renilla* luciferase activity. To compare the capacities of Runx2 and Runx3 in the transcriptional activation of *Ihh* promoter, the cDNA of *Runx2* or *Runx3* was inserted into pSG5, and *Runx2*$^{-/-}$ chondrocytes were transfected with DNA mixture containing p1313-luc (0.2 μg), *Runx2*- or *Runx3*-expressing vector or pSG5 (0.05 μg), and the control vector pRL-CMV (0.002 μg; Promega) using FuGENE 6 (Roche Diagnostics).

Acknowledgments

We thank M. Iwamoto for the *Sox9* probe; Z. Maruyama for helpful discussion; R. Fukuyama, N. Kanatani, A. Ono, and H. Enomoto for technical assistance; R. Hiraiwa for maintaining mouse colonies; and M. Yanagita for secretarial assistance. This work was supported by grants from the Ministry of Education, Culture, Sports, Science, and Technology, Japan.

The publication costs of this article were defrayed in part by payment of page charges. This article must therefore be hereby marked "advertisement" in accordance with 18 USC section 1734 solely to indicate this fact.

References

Akiyama, H., Chaboissier, M.C., Martin, J.F., Schedl, A., and de Crombrugghe, B. 2002. The transcription factor Sox9 has essential roles in successive steps of the chondrocyte differentiation pathway and is required for expression of Sox5 and Sox6. *Genes & Dev.* **16:** 2813–2828.

Bae, S.C., Takahashi, E., Zhang, Y.W., Ogawa, E., Shigesada, K., Namba, Y., Satake, M., and Ito, Y. 1995. Cloning, mapping and expression of PEBP2 αC, a third gene encoding the mammalian Runt domain. *Gene* **159:** 245–248.

Bi, W., Deng, J.M., Zhang, Z., Behringer, R.R., and de Crombrugghe, B. 1999. Sox9 is required for cartilage formation. *Nat. Genet.* **22:** 85–89.

Bitgood, M.J. and McMahon, A.P. 1995. Hedgehog and Bmp genes are coexpressed at many diverse sites of cell–cell interaction in the mouse embryo. *Dev. Biol.* **172:** 126–138.

Enomoto, H., Enomoto-Iwamoto, M., Iwamoto, M., Nomura, S., Himeno, M., Kitamura, Y., Kishimoto, T., and Komori, T. 2000. Cbfa1 is a positive regulatory factor in chondrocyte maturation. *J. Biol. Chem.* **275:** 8695–8702.

Enomoto, H., Shiojiri, S., Hoshi, K., Furuichi, T., Fukuyama, R., Yoshida, C., Kanatani, N., Nakamura, R., Mizuno, A., Zanma, A., et al. 2003. Induction of osteoclast differentiation by Runx2 through RANKL and OPG regulation and partial rescue of osteoclastogenesis in Runx2$^{-/-}$ mice by RANKL transgene. *J. Biol. Chem.* **278:** 23971–23977.

Enomoto, H., Furuichi, T., Zanma, A., Yamana, K., Yoshida, C., Sumitani, S., Yamamoto, H., Enomoto-Iwamoto, M., Iwamoto, M., and Komori, T. 2004. Runx2 deficiency in chondrocytes causes adipogenic changes in vitro. *J. Cell Sci.* **117:** 417–425.

Enomoto-Iwamoto, M., Enomoto, H., Komori, T., and Iwamoto, M. 2001. Participation of Cbfa1 in regulation of chondrocyte maturation. *Osteoarthritis Cartilage* **9:** S76–S84.

Gilbert, S.F. 1997. *Developmental Biology*, 5th ed., pp. 351–357. Sinauer Associates, Sunderland, MA.

Inada, M., Yasui, T., Nomura, S., Miyake, S., Deguchi, K., Himeno, M., Sato, M., Yamagiwa, H., Kimura, T., Yasui, N., et al. 1999. Maturational disturbance of chondrocytes in Cbfa1-deficient mice. *Dev. Dyn.* **214:** 279–290.

Inoue, K., Ozaki, S., Shiga, T., Ito, K., Masuda, T., Okado, N., Iseda, T., Kawaguchi, S., Ogawa, M., Bae, S.C., et al. 2002. Runx3 controls the axonal projection of proprioceptive dorsal root ganglion neurons. *Nat. Neurosci.* **5:** 946–954.

Iwamoto, M., Kitagaki, J., Tamamura, Y., Gentili, C., Koyama, E., Enomoto, H., Komori, T., Pacifici, M., and Enomoto-Iwamoto. M. 2003. Runx2 expression and action in chondrocytes are regulated by retinoid signaling and parathyroid hormone-related peptide (PTHrP). *Osteoarthritis Cartilage* **11:** 6–15.

Iwasaki, M., Le, A.X., and Helms, J.A. 1997. Expression of indian hedgehog, bone morphogenetic protein 6 and gli during skeletal morphogenesis. *Mech. Dev.* **69:** 197–202.

Jiménez, M.J., Balbin, M., Lopez, J.M., Alvarez, J., Komori, T., and Lopez-Otin, C. 1999. Collagenase 3 is a target of Cbfa1, a transcription factor of the runt gene family involved in bone formation. *Mol. Cell Biol.* **19:** 4431–4442.

Kim, I.S., Otto, F., Zabel, B., and Mundlos, S. 1999. Regulation of chondrocyte differentiation by Cbfa1. *Mech. Dev.* **80:** 159–170.

Komori, T. 2002. Runx2, a multifunctional transcription factor in skeletal development. *J. Cell. Biochem.* **87:** 1–8.

Komori, T., Yagi, H., Nomura, S., Yamaguchi, A., Sasaki, K., Deguchi, K., Shimizu, Y., Bronson, R.T., Gao, Y., Inada, M., et al. 1997. Targeted disruption of Cbfa1 results in a complete lack of bone formation owing to maturational arrest of osteoblasts. *Cell* **89:** 755–764.

Kundu, M., Javed, A., Jeon, J.P., Horner, A., Shum, L., Eckhaus, M., Muenk, M., Lian, J.B., Yang, Y., Nuckolls, G.H., et al. 2002. Cbfβ interacts with Runx2 and has a critical role in bone development. *Nat. Genet.* **32:** 639–644.

Levanon, D., Brenner, O., Negreanu, V., Bettoun, D., Woolf, E., Eilam, R., Lotem, J., Gat, U., Otto, F., Speck N., et al. 2001. Spatial and temporal expression pattern of Runx3 (Aml2) and Runx1 (Aml1) indicates non-redundant functions during mouse embryogenesis. *Mech. Dev.* **109:** 413–417.

Levanon, D., Bettoun, D., Harris-Cerruti, C., Woolf, E., Negreanu, V., Eilam, R., Bernstein, Y., Goldenberg, D., Xiao, C., Fliegauf, M., et al. 2002. The Runx3 transcription factor regulates development and survival of TrkC dorsal root ganglia neurons. *EMBO J.* **21:** 3454–3463.

Li, Q.L., Ito, K., Sakakura, C., Fukamachi, H., Inoue, K., Chi, X.Z., Lee, K.Y., Nomura, S., Lee, C.W., Han, S.B., et al. 2002. Causal relationship between the loss of RUNX3 expression and gastric cancer. *Cell* **109:** 113–124.

Miller, J., Horner, A., Stacy, T., Lowrey, C., Lian, J.B, Stein G., Nuckolls, G.H., and Speck N. 2002. The core-binding factor b subunit is required for bone formation and hematopoietic maturation. *Nat. Genet.* **32:** 645–649.

Okada, H., Watanabe, T., Niki, M., Takano, H., Chiba, N., Yanai, N., Tani, K., Hibino, H., Asano, S., Mucenski, M.L., et al. 1998. AML1(–/–) embryos do not express certain hematopoiesis-related gene transcripts including those of the PU.1 gene. *Oncogene* **17:** 2287–2293.

Okuda, T., van Deursen, J., Hiebert, S.W., Grosveld, G., and Downing, J.R. 1996. AML1, the target of multiple chromosomal translocation in human leukemia, is essential for normal fetal liver hematopoiesis. *Cell* **84:** 321–330.

Otto, F., Thornell, A.P., Crompton, T., Denzel, A., Gilmour, K.C., Rosewell, I.R., Stamp, G.W.H., Beddington, R.S.P., Mundlos, S., Olsen, B.R., et al. 1997. Cbfa1, a candidate gene for cleidocranial dysplasia syndrome, is essential for osteoblast differentiation and bone development. *Cell* **89:** 765–771.

St-Jacques, B., Hammerschmidt, M., and McMahon, A.P. 1999. Indian hedgehog signaling regulates proliferation and differentiation of chondrocytes and is essential for bone formation. *Genes & Dev.* **13:** 2072–2086.

Stricker, S., Fundele, R., Vortkamp, A., and Mundlos, S. 2002. Role of Runx genes in chondrocyte differentiation. *Dev. Biol.* **245:** 95–108.

Takahashi, Y., Rayman, J.B., and Dynlacht BD. 2000. Analysis of promoter binding by the E2F and pRB families in vivo: Distinct E2F proteins mediate activation and repression. *Genes & Dev.* **14:** 804–16.

Takamoto, M., Tsuji, K., Yamashita, T., Sasaki, H., Yano, T., Taketani, Y., Komori, T., Nifuji, A., and Noda, M. 2003. Hedgehog signaling enhances core-binding factor a1 and receptor activator of nuclear factor-κB ligand (RANKL) gene expression in chondrocytes. *J. Endocrinol.* **177:** 413–421.

Takeda, S., Bonnamy, J.P., Owen, M.J., Ducy, P., and Karsenty, G. 2001. Continuous expression of Cbfa1 in nonhypertrophic chondrocytes uncovers its ability to induce hypertrophic chondrocyte differentiation and partially rescues Cbfa1-deficient mice. *Genes & Dev.* **15:** 467–481.

Ueta, C., Iwamoto, M., Kanatani, N., Yoshida, C., Liu, Y., Enomoto-Iwamoto, M., Ohmori, T., Enomoto, H., Nakata, K., Takada, K., et al. 2001. Skeletal malformations caused by overexpression of Cbfa1 or its dominant negative form in chondrocytes. *J. Cell Biol.* **153:** 87–99.

Vortkamp, A., Lee, K., Lanske, B., Segre, G.V., Kronenberg, H.M., and Tabin, C.J. 1996. Regulation of rate of cartilage differentiation by Indian hedgehog and PTH-related protein. *Science* **273:** 613–622.

Wang, Q., Stancy, T., Binder, M., Marín-Padilla, M., Sharpe, A.H., and Speck, N.A. 1996. Disruption of the Cbfa2 gene causes necrosis and hemorrhaging in the central nervous system and blocks definitive hematopoiesis. *Proc. Natl. Acad. Sci.* **93:** 3444–3449.

Yoshida, C.A., Furuichi, T., Fujita, T., Fukuyama, R., Kanatani, N., Kobayashi, S., Satake, M., Takada, K., and Komori, T. 2002. Core-binding factor β interacts with Runx2 and is required for skeletal development. *Nat. Genet.* **32:** 633–638.

Zou, H., Wieser, J., Massage, J., and Niswander, L. 1997. Distinct roles of types I bone morphogenetic protein receptors in the formation and differentiation of cartilage. *Genes & Dev.* **11:** 2191–2203.